ACS Chemical Neuroscience

Research Article

pubs.acs.org/chemneuro

Calmodulin Transduces Ca^{2+} Oscillations into Differential Regulation of Its Target Proteins

Nikolai Slavov,[†,∥] Jannette Carey,[‡] and Sara Linse*[,§]

[†]Department of Molecular Biology and [‡]Department of Chemistry, Princeton University, Princeton, New Jersey 08544, United States
[§]Department of Biochemistry and Structural Biology, Lund University, Lund, Sweden

Supporting Information

ABSTRACT: Diverse physiological processes are regulated differentially by Ca^{2+} oscillations through the common regulatory hub calmodulin. The capacity of calmodulin to combine specificity with promiscuity remains to be resolved. Here we propose a mechanism based on the molecular properties of calmodulin, its two domains with separate Ca^{2+} binding affinities, and target exchange rates that depend on both target identity and Ca^{2+} occupancy. The binding dynamics among Ca^{2+}, Mg^{2+}, calmodulin, and its targets were modeled with mass-action differential equations based on experimentally determined protein concentrations and rate constants. The model predicts that the activation of calcineurin and nitric oxide synthase depends nonmonotonically on Ca^{2+}-oscillation frequency. Preferential activation reaches a maximum at a target-specific frequency. Differential activation arises from the accumulation of inactive calmodulin-target intermediate complexes between Ca^{2+} transients. Their accumulation provides the system with hysteresis and favors activation of some targets at the expense of others. The generality of this result was tested by simulating 60 000 networks with two, four, or eight targets with concentrations and rate constants from experimentally determined ranges. Most networks exhibit differential activation that increases in magnitude with the number of targets. Moreover, differential activation increases with decreasing calmodulin concentration due to competition among targets. The results rationalize calmodulin signaling in terms of the network topology and the molecular properties of calmodulin.

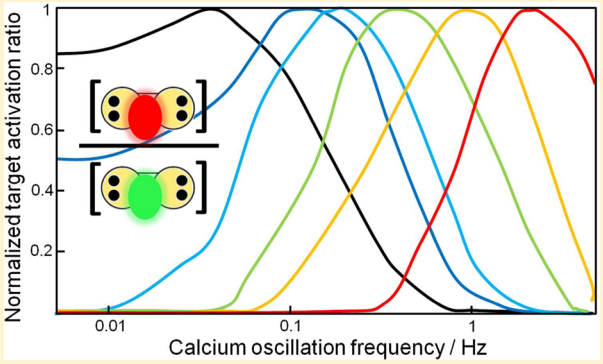

KEYWORDS: *Signal transduction, oscillatory dynamics, frequency dependence, ligand binding, cooperativity, tuning, emergent property*

A wide variety of external stimuli induce transient elevations in cytoplasmic Ca^{2+} concentrations, via intake through gated channels or by mobilization of endoplasmic reticulum stores. Ca^{2+} transients typically occur in series (oscillations) and vary in amplitude, duration, and frequency. Experimental data suggest that the temporal and spatial dynamics of Ca^{2+} transients contribute to specificity and sensitivity in regulation of a diverse range of physiological processes.[1−4] Many Ca^{2+}-regulated processes, for example, cardiac and neuronal rhythms,[5] are sensitive to temporal dynamics, including activation of some processes and simultaneous down-regulation of others.[5−7] This pattern implies the existence of global mechanisms that transduce the information encoded in the common Ca^{2+} oscillations into distinct cellular responses. This important question has been addressed by experiments and models that explore mechanisms of frequency-dependent regulation based on local concentration gradients of $[Ca^{2+}]$.[3,8−10] These models show that indeed slow diffusion of calcium can result in local microdomains of high $[Ca^{2+}]$; the higher the frequency of calcium oscillation, the higher the microdomain $[Ca^{2+}]$ and the activity of all targets in the microdomain.

Ca^{2+}-binding proteins, most prominently calmodulin (CaM), regulate downstream functions in response to Ca^{2+}. CaM is a promiscuous regulator with several hundred targets known to date, including kinases, phosphatases, cytoskeletal proteins, synaptic proteins, cell cycle proteins, ion channels, and the buffer proteins that regulate intracellular Ca^{2+} stores.[11−25] The central importance of the molecular structure of CaM is underscored by its identical sequence in all vertebrates,[26,27] and the observation that the *Drosophila* point mutants investigated to date are lethal.[28] It has been unclear, however, how the molecular properties of CaM can enable a single regulatory hub to differentially activate targets in response to the common signal of Ca^{2+} flux.

The molecular properties of CaM appear compatible with a direct role in temporal response to Ca^{2+} oscillations. Here, a biophysical model is developed that incorporates explicitly CaM ligand-binding dynamics to explore whether the promiscuity of CaM could be rationalized if it were the locus of global regulation. CaM contains four EF-hands, each binding

Received: November 30, 2012
Accepted: January 21, 2013
Published: January 21, 2013

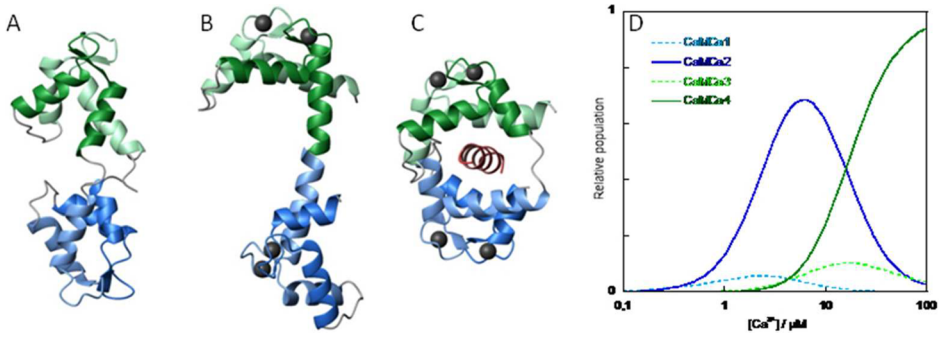

Figure 1. Calmodulin. (A) NMR structure of apo calmodulin (1cfc.pdb), (B) X-ray structure of CaM-Ca_4 (1cll.pdb) and (C) crystal structure of CaM-Ca_4 peptide complex (1cdl.pdb). Panels A–C were prepared using MOLMOL[75] with EF1 in light green, EF2 in green, EF3 in light blue, and EF4 in blue. Ca^{2+} ions are shown as black balls and the target peptide in red. (D) Fraction of calmodulin with one (light blue, dashed), two (blue), three (light green, dashed), and four (green) Ca^{2+} bound as a function of free Ca^{2+} concentration at physiological KCl concentration based on experimental binding constants.[31]

one Ca^{2+} ion, that are organized as pairs in two globular domains connected by a flexible tether (Figure 1).[29,30] Pairing of the EF-hands allows each domain to bind two Ca^{2+} ions with positive cooperativity;[31,32] thus, species with zero, two, or four Ca^{2+} ions bound dominate over those with one or three Ca^{2+} (Figure 1D). The domains display distinct ion affinities and kinetics, with approximately 6-fold higher Ca^{2+} affinity[31] and ~10-fold lower Ca^{2+} off-rates (24 vs 240 s^{-1}; ref 33) in the C-terminal domain than in the N-terminal domain at physiological salt concentration. Mg^{2+} is a potent physiological competitor with Ca^{2+} for CaM binding despite much lower affinity (K_D = 1.5–6 mM for Mg^{2+} and K_D = 0.05–15 μM for Ca^{2+} depending on ionic strength[31,34−36]) due to its much higher cytoplasmic concentration (0.5–2 mM[34,37]). Its opposite domain preference sets up competition at the N-terminal domain that can make Mg^{2+} dissociation rate-limiting for response to Ca^{2+}. Taking these properties into account and modeling the formation and dissociation of active complex may capture essential biologically important dynamics in the activation of CaM targets.

The two domains of CaM cooperate in target binding[38−40] (Figure 1C). Their flexible linkage allows the domains to take many orientations relative to one another,[41] as the electrostatic repulsion between the Ca^{2+}-bound domains is largely screened at physiological salt.[42−44] The prevalence of methionine side-chains at the hydrophobic pockets allows for optimization of van der Waals and steric interactions with a variety of targets.[25,45] These factors equip CaM with a wide substrate tolerance and high affinity.[29,30,46] Thus, calmodulin combines high specificity in folding and EF-hand pairing[47,48] with a remarkable promiscuity in target recognition. Most CaM targets have highest affinity for, and are activated only by, CaM with four Ca^{2+} ions bound. Due to thermodynamic linkage, target binding increases the affinity of CaM for Ca^{2+}, but at basal Ca^{2+} concentrations (~0.1 μM) a significant fraction of CaM-target complexes have only two bound Ca^{2+} ions.[37] Although CaM is abundant in all eukaryotic cells (~2–20 μM[49,50]), the very large number of targets could make it stoichiometrically limiting in some conditions. In the present work, simulation of model networks with experimentally constrained rate constants and concentrations was used to investigate whether ligand binding dynamics in the CaM network can result in frequency-specific CaM target activation.

RESULTS

Network Model. To explore the role of ligand binding dynamics in the CaM network, the binding interactions among Ca^{2+}, CaM, and target proteins were modeled with differential (eqs 1–5) and mass-balance (eqs 6–8) equations. Importantly, eqs 1–5 can account explicitly for the dynamics of formation and dissociation of intermediary species that are commonly neglected. Solving these equations numerically describes the species distribution and rates of conversion among species in response to trains of Ca^{2+} transients with defined frequency and durations. A first set of simulations modeled a small network with only two targets, containing in total 12 different species (Figure 2). Calcineurin (CN) and nitric oxide synthase (NOS) were chosen as model target proteins because of the availability of experimental rate constants with divergent ranges (Table 1). This small network was used to determine how the distribution

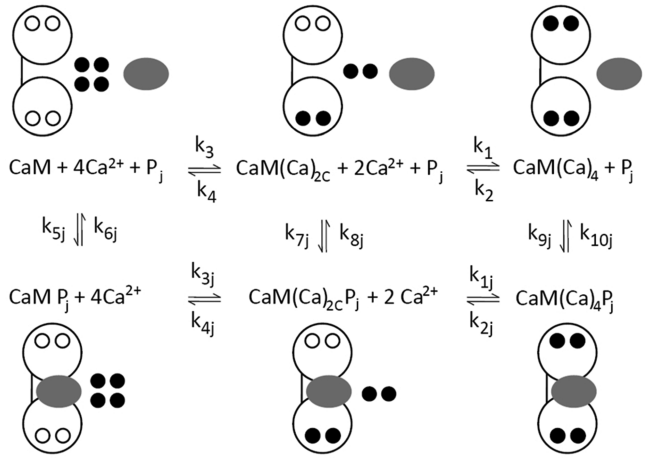

Figure 2. Network model. Reactions and species taken into account in the simulations are shown. Calmodulin (CaM) is shown as a dumbbell indicating its two-domain structure, open circles denote unoccupied Ca^{2+}-binding sites, filled black circles are Ca^{2+} ions, and the gray oval denotes the *j*th target protein. The subscript 2C indicates two Ca^{2+} ions in the C-terminal domain of calmodulin, and subscript *j* indicates the *j*th target protein. The top line cartoon and reactions indicate stepwise reversible binding of pairs of Ca^{2+} ions to calmodulin. The bottom line cartoon and reactions indicate stepwise reversible binding of pairs of Ca^{2+} ions to calmodulin in complex with the *j*th target protein. The vertical reactions indicate reversible binding of the *j*th target.

dx.doi.org/10.1021/cn300218d | ACS Chem. Neurosci. 2013, 4, 601–612

Table 1. Rate Constants for CN and NOS[a]

	Ca^{2+} binding		target binding		
	$k_a/\mu M^{-2}\ s^{-1}$	k_d/s^{-1}	$k_a/\mu M^{-1}\ s^{-1}$	k_d/s^{-1}	refs
CaM	$k_1 = 65$	$k_2 = 850$			
	$k_3 = 6$	$k_4 = 12$			26, 52
CaM CN	$\underline{k_{11} = 65}$	$k_{21} = 425$	$k_{51} = 46$	$k_{61} = 348$	
	$\underline{k_{31} = 6}$	$k_{41} = 0.06$	$k_{71} = 46$	$k_{81} = 0.008$	
			$k_{91} = 46$	$k_{101} = 0.0012$	45, 51
CaM NOS	$\underline{k_{12} = 65}$	$k_{22} = 116$	$k_{52} = 0.13$	$k_{62} = 2.1$	
	$\underline{k_{32} = 60}$	$k_{42} = 1$	$k_{72} = 0.13$	$k_{82} = 0.0013$	
			$k_{92} = 0.13$	$k_{102} = 2.5 \times 10^{-5}$	42, 43, 52

[a]The rate constants for CN and NOS are marked with subindices 1 and 2, respectively, and are according to Figure 2. The association rate constants are designated as k_a and have units of $\mu M^{-2}\ s^{-1}$ for the association of Ca^{2+} ions (which was modeled as trimolecular; for justification, see Supporting Information Figure S4) and $\mu M^{-1}\ s^{-1}$ for the association of the targets. The dissociation rate constants are designated as k_d and have units of s^{-1}. The constants inferred from the thermodynamic cycles in Supporting Information Figure S2 are underlined.

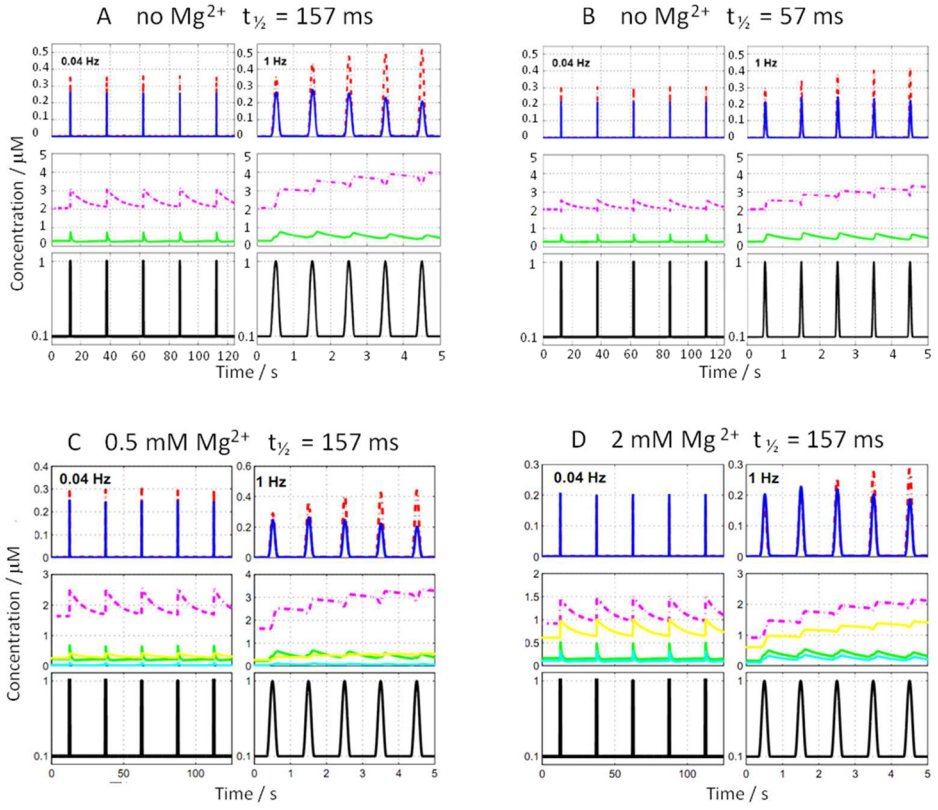

Figure 3. Activation of CN and NOS by Ca^{2+} oscillations. Concentrations of network species are shown as a function of time under different simulation conditions. The Mg^{2+} concentration and the midheight duration of Ca^{2+} transients are given above each set of panels (A–D). Within each set of panels, the top panels show active species with $CaM(Ca)_4CN$ in red and $CaM(Ca)_4NOS$ in blue; the middle panels show inactive intermediates with $CaM(Ca)_{2C}CN$ in magenta, $CaM(Ca)_{2C}NOS$ in green, $CaM(Ca)_{2C}(Mg)_{2N}CN$ in yellow, and $CaM(Ca)_{2C}(Mg)_{2N}NOS$ in cyan. The bottom panels show the concentration of free Ca^{2+} (black), oscillating at low frequency (0.04 Hz; left) and at high frequency (1 Hz; right).

of species varies over time in response to defined Ca^{2+}-oscillation profiles differing in frequency and duration of Ca^{2+} transients in the presence and absence of competing Mg^{2+} ions.

Low versus High Frequency of Ca^{2+} Transients. Figure 3A shows the results of simulations of networks including CaM, Ca^{2+}, NOS, and CN at two frequencies of Ca^{2+} transients. Such trains of Ca^{2+} transients with similar midwidth duration are commonly measured in nonexcitable cells, such as hepatocytes.[6] At low frequency (0.04 Hz, Figure 3A, top left panel), the formation and decay of active complexes (i.e., $CaM(Ca)_4CN$ and $CaM(Ca)_4NOS$) closely trace the Ca^{2+} transients. The concentration of active CN complex is greater than that of NOS during each spike, reflecting their differences in affinity, but all spikes result in equivalent extents of activation because the intertransient intervals (25 s) are long enough for all network species to return to their equilibrium concentrations between spikes. In contrast, at high frequency (1 Hz), the intertransient periods are too short (<1 s) to allow for complete relaxation to equilibrium values, and activation of both target proteins becomes hysteretic (Figure 3A, top right

dx.doi.org/10.1021/cn300218d | ACS Chem. Neurosci. 2013, 4, 601–612

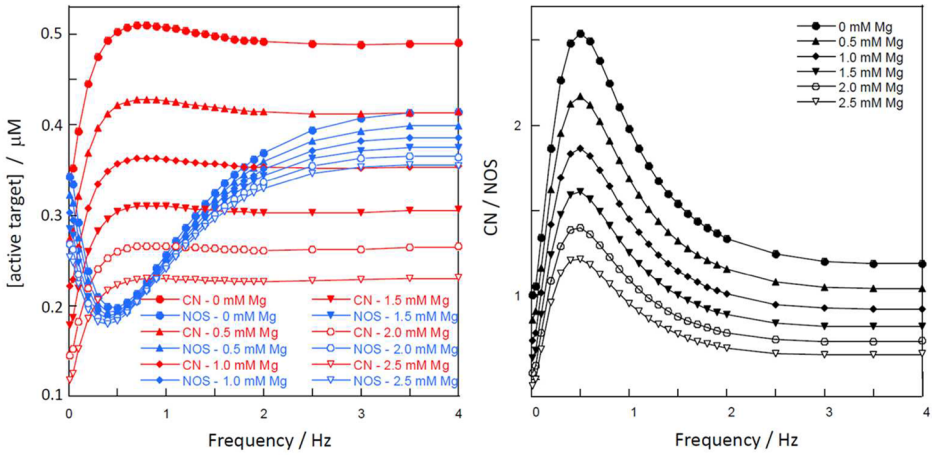

Figure 4. Frequency dependence of CN and NOS activity. (Left) Concentration of active target CN ($CaM(Ca)_4CN$ in red) and NOS ($CaM(Ca)_4NOS$ in blue) and (right) ratio of concentrations of active species ($CaM(Ca)_4CN$ over $CaM(Ca)_4NOS$) on the 11th transient as a function of Ca^{2+} frequency. Data at the following Mg^{2+} concentrations are shown: 0 mM (filled circle), 0.5 mM (filled upward triangle), 1.0 mM (filled diamond), 1.5 mM (filled downward triangle), 2.0 mM (open circle), and 2.5 mM (open triangle).

panel). The response to the first transient is identical at both frequencies, but the amplitude of response to subsequent Ca^{2+} spikes differs. CN becomes more activated on each spike (asymptotically approaching a maximum) and NOS becomes less active on each spike (asymptotically approaching a minimum).

This response is found to depend on the extent to which CaM is redistributed among $CaM(Ca)_{2C}CN$, $CaM(Ca)_{2C}NOS$, and free CaM during the intertransient period (Figure 3A middle), governed by the association and dissociation rates. Depending on the frequency of transients, inactive intermediate CaM-target complexes with two Ca^{2+} ions bound may accumulate between transients. Since binding of Ca^{2+} to the C-domain of free CaM is slow relative to the duration of individual transients,[51] activation of CaM target protein P_j is proportional to $CaM(Ca)_{2C}P_j$ at the beginning of the Ca^{2+} transients. Thus, slow redistribution makes the activation of CaM targets dependent on the timing of Ca^{2+} transients. Differential activation emerges due to the accumulation of inactive intermediate states and the variation among targets in the rate constants for formation and dissociation of these intermediates. Therefore, the introduction of explicit terms for the intermediary states (eqs 1−5) allows capturing important dynamics that are missed by simpler models. The rate constants in the CaM-Ca^{2+}-target protein network thus permit some target complexes to accumulate, leading to sequestration of CaM, suppression of other target(s), and preferential activation. Therefore, increased frequency can also lead to deactivation for some targets, as observed for NOS (Figure 3). This activation mechanism allows for truly differential regulation, not simply monotonically increasing activation with increasing frequency.

Frequency Dependence. To evaluate the frequency dependence of the observed differential regulation over a wider range of frequencies, simulations with 11 transients of 157 ms duration were carried out for the model network including CN and NOS at 28 frequencies ranging from 0.01 to 5 Hz (data up to 4 Hz shown in Figure 4). The concentration of each active species, $CaM(Ca)_4CN$ or $CaM(Ca)_4NOS$, at the 11th transient is shown as a function of frequency in Figure 4, left, and the ratio of the concentrations the two active forms in Figure 4, right. There is not a discrete frequency at which behavior switches from equal response to each transient to altered response to subsequent transients. Rather there is a progressive change in behavior starting already in the very low frequency end (compare first two points in Figure 4). However, around 0.5 Hz, the discrimination between CN and NOS reaches a maximum. This optimum reflects the largest amplification of CN activation and largest suppression of NOS activation around 0.5 Hz. This difference is maintained in the presence of physiological concentrations of Mg^{2+}, although its magnitude diminishes (Figure 4, right) and the peak shifts very slightly to lower frequency values. At frequencies above ~3 Hz, no difference in the ratio of active species is detected because transients are too rapid to permit species redistribution between spikes. These results suggest that the level of differential activation is largest when the frequency of Ca^{2+} oscillations is tuned to rates in the system that allow for efficient resonance with the frequency.

Duration of Ca^{2+} Transients. Typical durations of transients range from a few milliseconds in excitable cells to around 1 s.[6,52] Networks including CaM, Ca^{2+}, NOS, and CN were simulated with two durations of the Ca^{2+} transients (midheight duration 57 or 157 ms) at frequencies of 0.04 and 1 Hz. As expected, longer transients (midheight duration 157 ms, Figure 3A) result in longer durations of activation for both CN and NOS as compared to shorter transients (57 ms, Figure 3B). Shorter transients lead to a lower level of formation of active species during the transient, and lower intermediate concentration between transients. However, the amplitudes of activation for CN and NOS respond differentially to the change in duration of Ca^{2+} transients. This is seen mainly at the higher frequency (compare Figure 3A and B, top right panels). Decreasing the duration decreases the amplitude of activation of CN while slightly increasing the amplitude of NOS activation. This reduction is seen mainly for the more slowly dissociating $CaM(Ca)_{2C}CN$ that gives CN less chance to suppress NOS with short transients and the competition is reduced.

Wider Range of Rate Constants. Other combinations of rate constants besides those estimated from experiment for CN and NOS were evaluated to determine the range of values that could lead to target discrimination and a frequency optimum. A set of 2500 hypothetical networks of two targets was generated by picking at random rate constants within the ranges given in

dx.doi.org/10.1021/cn300218d | ACS Chem. Neurosci. 2013, 4, 601−612

Table 2 and protein concentrations in the range 1−100 μM as observed experimentally.[14] The tabulated rate constants span many orders of magnitude and encompass all values estimated for the CaM targets that have been studied experimentally, representing affinity variations over 7−9 orders of magnitude. Simulation of each of the 2500 networks was performed with 11 Ca^{2+} transients of 157 ms duration at 28 frequencies between 0.005 and 5 Hz. Figure 5 shows results for the first 50 networks, which are representative of the simulated set. The ratio of the concentrations of the two active species, $CaM(Ca)_4P_1$ and $CaM(Ca)_4P_2$, at the 11th transient is normalized to facilitate comparison. For almost all pairs, the data reveal differential regulation and distinct frequency dependence with an optimum within the studied frequency range. Furthermore, the optimum frequency varies considerably among pairs of hypothetical targets. This behavior indicates that if several targets are part of the same network, activation of different groups of targets may occur at different frequencies.

Table 2. Rate Constant Limits for Generic Target Proteins[a]

	Ca^{2+} binding		target binding	
	$k_a/\mu M^{-2}\ s^{-1}$	k_d/s^{-1}	$k_a/\mu M^{-1}\ s^{-1}$	k_d/s^{-1}
lower limit	$k_{1j} = 1$	$k_{2j} = 1$	$k_{5j} = 0.1$	$k_{6j} = 1 \times 10^{-4}$
	$k_{3j} = 0.1$	$k_{4j} = 0.001$	$k_{7j} = 0.1$	$k_{8j} = 1 \times 10^{-4}$
			$k_{9j} = 0.1$	$k_{10j} = 1 \times 10^{-6}$
upper limit	$k_{1j} = 1000$	$k_{2j} = 1000$	$k_{5j} = 100$	$k_{6j} = 100$
	$k_{3j} = 100$	$k_{4j} = 10$	$k_{7j} = 100$	$k_{8j} = 1$
			$k_{9j} = 100$	$k_{10j} = 0.1$

[a]Limits for randomly generated rate constants. All notations and units are the same as in Table 1 and according to Figure 2.

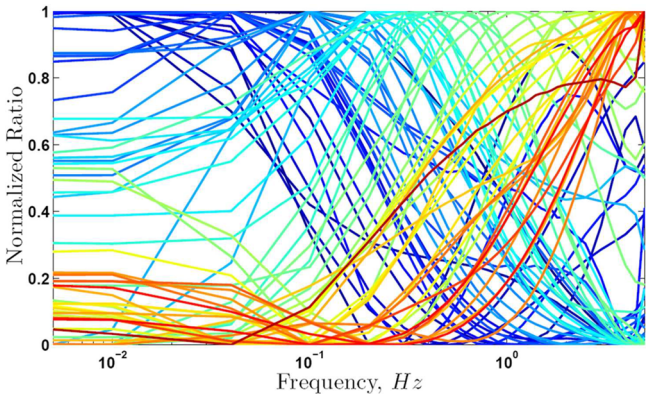

Figure 5. Frequency dependence in generalized networks. Ratio of active targets in a network of two targets using parameters picked randomly within the ranges in Table 2, and calmodulin concentration in the range 1−100 μM. The Ca^{2+} train consisted of 11 transients with 157 ms midheight duration and simulations were performed at Ca^{2+} oscillation frequency ranging from 0.005 to 5 Hz. Each curve represents one pair of targets and the different colors are used only to facilitate viewing of the curves.

Networks with Higher Numbers of Targets. To evaluate the effect of increasing the number of targets in a network, simulations were carried out for three sizes of hypothetical networks containing two, four, or eight targets. Protein concentrations were picked at random within the experimentally observed range 1−100 μM,[14] and rate constants were varied over 3−6 orders of magnitude within the ranges given in Table 2 to generate 10 000 parameter sets for each network size. All networks were simulated at frequencies of 0.04 and 1 Hz with Ca^{2+} trains of 11 transients with midheight duration of 157 ms. To compare the level of differential target activation between networks with different numbers of targets, two metrics, ΔP_j and ΔA, are introduced. ΔP_j measures the fold change in activation of one target at two frequencies. ΔA averages ΔP_j over all targets in the network (see eqs 13 and 14 in the Methods section).

For networks of two targets, 92% of the simulated networks yield frequency-dependent activation of target proteins as judged by ΔA values (Figure 6A). For the remaining 8% of parameter sets, ΔA is close to 1, implying no frequency dependence. The fraction of parameter sets yielding frequency-dependent activation (frequency dependence of both ΔP_j and ΔA) increases with the number of targets, and already with four targets this fraction is >99%. This behavior is also evident in Figure 6A as distributions shifted toward higher ΔA values when more targets are present in the networks. The networks with 2, 4, and 8 targets proteins have mean ΔA values of 1.58, 2.0, and 2.4, respectively. This trend suggests that inclusion of even more targets will lead to further increase in ΔA. The dispersion of the distribution also decreases with the number of targets. The shifting and narrowing indicate that the number of

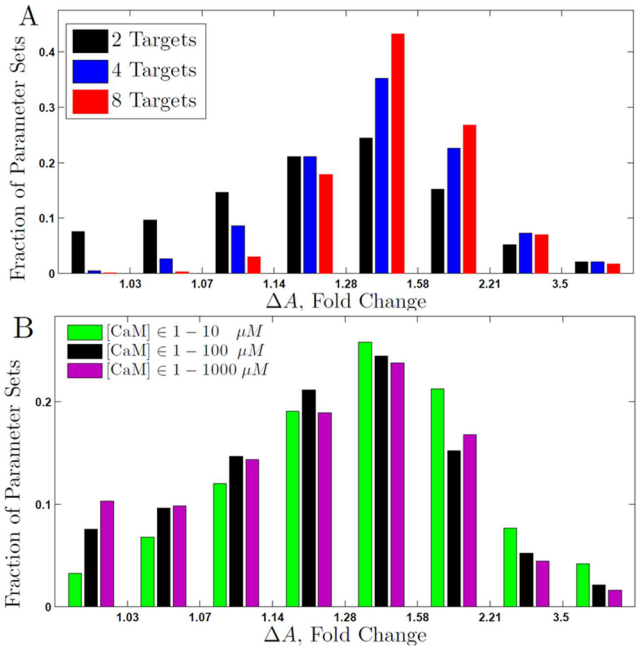

Figure 6. Differential activation in generalized networks. Distribution of ΔA values among 10 000 simulations for generalized networks with rate constants generated at random within the ranges given in Table 2. ΔA is calculated comparing 1 and 0.04 Hz oscillations, and the fractions of simulations yielding the indicated ranges of ΔA values are shown. The simulations used trains of 11 Ca^{2+} transients with 157 ms midheight duration without Mg^{2+}. (A) Effect of number of targets. ΔA distributions for networks of two (black), four (blue), or eight (red) targets. The calmodulin concentration was chosen randomly in the range 1−100 μM, and the total target concentration in the range 1−100 μM. (B) Effect of limiting calmodulin concentration. Distribution of ΔA values for networks containing two targets and calmodulin concentration sampled in the ranges 1−10 μM (green), 1−100 μM (black), or 1−1000 μM (magenta).

dx.doi.org/10.1021/cn300218d | ACS Chem. Neurosci. 2013, 4, 601−612

parameter combinations yielding higher ΔA values is larger when more targets are present in the network. This effect reflects the fact that with more targets, the likelihood is higher that some will have rate constants supporting differential activation between 0.04 and 1 Hz oscillations, that is, having rate constants that allow efficient coupling with the frequency in this range.

Replotting the graph in Figure 6A for a randomly chosen subset of 6000 simulated parameters from each set shows convergence to the same distribution of ΔA (not shown), indicating that the number of simulated sets is large enough to be representative of calmodulin network behavior over the studied ranges of rate constants. The 100 sets of rate constants that resulted in the smallest or largest differential responses (lowest or highest ΔA values, respectively) are distributed over the whole parameter space (Supporting Information Figure S1). Thus, differential activation of CaM targets depends on the frequency of Ca^{2+} oscillations for a very wide range of rate constant values.

Competition from Mg^{2+}. Even though binding of Mg^{2+} to CaM does not lead directly to target activation, Mg^{2+} competes with Ca^{2+} for binding to CaM and, thus, influences target activation.[35] Mg^{2+} has opposite domain preferences for CaM, and the complexes $CaM(Ca)_{2C}(Mg)_{2N}P_j$ may influence target activation since dissociation of Mg^{2+} may be slower than the association of Ca^{2+}.[35] The role of Mg^{2+} was investigated by repeating the simulations of the networks containing CN and NOS at 28 different frequencies ranging from 0.01 to 5 Hz in the presence of 0.5, 1, 1.5, 2, or 2.5 mM Mg^{2+}. Inclusion of Mg^{2+} expands the network from 12 to 19 species and adds four new rate constants. The new species are Mg^{2+}, $CaM(Mg)_{2N}$, $CaM(Mg)_4$, $CaM(Ca)_{2C}(Mg)_{2N}NOS$, $CaM(Ca)_{2C}(Mg)_{2N}CN$, $CaM(Mg)_4NOS$, and $CaM(Mg)_4CN$, whereas $CaM(Mg)_{2C}(Ca)_{2N}CN$ and $CaM(Mg)_{2C}(Ca)_{2N}NOS$ are omitted, as their concentrations will under all circumstances be negligible due to opposite ion preferences of the domains.

Examples of simulations at 0.04 and 1 Hz are shown in Figure 3 at 0.5 mM Mg^{2+} (Figure 3C) and 2 mM Mg^{2+} (Figure 3D). The inclusion of Mg^{2+} affects the level of activated CN much more than NOS over the entire frequency range (data up to 4 Hz shown in Figure 4). The concentration of $CaM(Ca)_4CN$ at the 11th transient is reduced in the presence of Mg^{2+} and shows an almost linear dependence on Mg^{2+} concentration, whereas the concentration of $CaM(Ca)_4NOS$ is largely independent of Mg^{2+} concentration (Figure 4A). In the presence of 1−2.5 mM Mg^{2+}, CN is more activated than NOS around 0.5 Hz, whereas at both lower and higher frequencies NOS is more activated than CN. Suppression of CN reduces the ratio of $CaM(Ca)_4CN$ to $CaM(Ca)_4NOS$ over the whole frequency range. Still, the ratio shows a peak around 0.5 Hz at all Mg^{2+} concentrations tested (Figure 4B), indicating a frequency-dependent difference in activation of the targets in the presence of biologically relevant concentrations of Mg^{2+}.

Calmodulin Concentration. The role of CaM concentration was first evaluated by performing a series of single simulations with 10 μM NOS and 10 μM CN and the CaM concentration set to 1, 2, 5, 10, 20, 50, or 100 μM. When the CaM concentration is lower than the total target concentration, these simulations show a higher level of differential activation with suppression of NOS (data not shown), suggesting sequestration of CaM in $CaM(Ca)_4CN$ complexes. Thus, competition for limited CaM leads simultaneously to preferential activation of one target and suppression of the other, implying a mechanism for truly differential regulation, rather than monotonically increasing activation.

The role of CaM concentration was further evaluated by generating 10 000 networks of two targets for each of three concentration ranges of CaM (1−10, 1−100, and 1−1000 μM). Rate constants were selected randomly within the ranges given in Table 2, and concentrations of target proteins in the range 1−100 μM. Figure 6B shows the ΔA distributions for the three CaM concentration ranges. A shift of the distribution to higher ΔA values is seen for networks with CaM concentrations sampled in the range 1−10 μM compared to 1−100 μM, and there is a small shift in the same direction also when 1−100 μM is compared to 1−1000 μM. This indicates that the frequency dependence increases as the CaM concentration range becomes more limited. Although differential activation is maintained even when the concentration of CaM exceeds the total concentration of all targets, it is strongest when CaM is stoichiometrically limiting, as is thought to be the case in vivo.[14]

Sensitivity Analysis. A sensitivity analysis was carried out for networks with two targets to investigate which parameters are most critical for the appearance of differential activation and to evaluate potential interdependence of parameters. Partial correlations between ΔA and each parameter and between ΔA and each pair of parameters (not shown) were computed based on 10 000 generated networks with protein concentrations in the range 1−100 μM and rate constants in the ranges given in Table 2. The absolute value of each partial correlation is proportional to the influence of the corresponding parameter on ΔA, and its sign indicates whether the influence is negative or positive (see Methods). A negative partial correlation is found between ΔA and the CaM concentration (Figure 7), in agreement with the finding that low CaM concentrations are associated with increased competition between targets. Consistent with the interpretation of the results in Figure 3, the rate constants for association and dissociation of Ca^{2+} at the C-terminal domain of target-bound CaM, k_{3j} and k_{4j}, have the

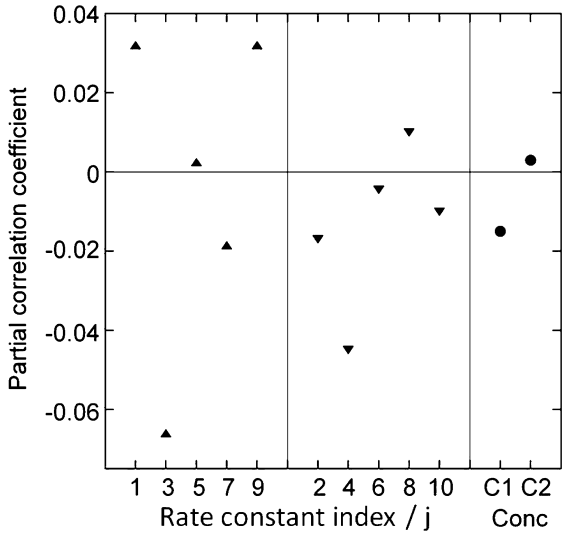

Figure 7. Sensitivity analysis. Partial correlation coefficient between ΔA and each varied parameter for 10 000 simulations of networks having two targets and no magnesium. The rate constants k_{ij} (indicated by their indices i) are displayed as upward triangle (association rate constants) or downward triangle (dissociation rate constants) and concentrations as filled circles (C1 = total calmodulin concentration, C2 = target concentration).

dx.doi.org/10.1021/cn300218d | ACS Chem. Neurosci. 2013, 4, 601−612

strongest influence on ΔA, with low values for these rate constants associated with high values of ΔA. This is seen as a negative partial correlation between ΔA and these rate constants (Figure 7). Target proteins for which these rate constants are low have slowly evolving intermediate complexes, leading to enhanced differential activation. Other association rate constants are more weakly correlated with ΔA, either positively (k_{1j} and k_{9j}) or negatively (k_{7j}) except for k_{5j} that is uncorrelated. All dissociation rate constants except k_{8j} are negatively correlated with ΔA, meaning that on average low dissociation rate constants favor high ΔA. The results of the sensitivity analysis thus imply that differences in rates among the intermediate complexes provide the network with frequency dependence and lead to differential activation of targets. The pairwise sensitivity analysis points to a number of interdependencies (data not shown). For example, a synergistic effect is seen between k_{7j} and k_{8j}, suggesting that ΔA increases with the rate of exchange between free target and target bound to CaM with a Ca^{2+}-saturated C-terminal domain. The finding that nearly all rate constants display partial correlation to ΔA and thus contribute to differential regulation suggests that the observed differential activation is an emergent property of the whole network rather than a property arising from the superposition of a few individual interactions.

DISCUSSION

The mechanism described here makes it possible, based on temporal dynamics alone, for a Ca^{2+}-calmodulin signaling network to decode the information in spike timing to distinguish among different cellular pathways that use Ca^{2+} as a common second messenger. The calmodulin signaling network is thus a striking example of the importance of kinetic discrimination in a system of multiple competing interactions. Both the relative rates of different reactions and the rates of the reactions relative to the timing of the signaling event set up the selectivity among branches of the network. The network is dynamically driven if the intertransient intervals are shorter than the time required for equilibration of the slowest steps in the network. Therefore, the activation of CaM targets is determined by kinetics rather than by affinities except at very low Ca^{2+} oscillation frequencies.

Kinetic Discrimination. Kinetic competition may arise from differences in association and/or dissociation rates. Association rate differences have, for example, been invoked to explain competition in DNA binding,[53] whereas protein folding may rely on longer average lifetime of native relative to non-native contacts.[54] For the calmodulin signaling network, differences in both association and dissociation rate constants are found to contribute to differential activation. Differential activation requires that the rates of some binding reactions are low relative to the frequency of the Ca^{2+} signaling event. Low dissociation rates of some complexes lead to accumulation of intermediates between transients, leading both to fast activation of those targets and suppressed activation of other targets. With intermediates at low concentrations association rates may become slow and rate limiting. High association rates of some targets can deplete CaM and limit association rates of other reactions.

Role of Intermediates. One mechanism for differential activation found here relies on the buildup of the $CaM(Ca)_{2C}P_j$ species between transients. Most targets in complexes with CaM having only two Ca^{2+} ions bound are inactive, and the slow dissociation of $CaM(Ca)_{2C}P_j$ reflects the high stability of such complexes. Many Ca^{2+}-activated CaM targets, such as CaN, NOS, myosin light-chain kinase, CaM kinase II, and Ca-ATPase are indeed known to form very stable complexes with Ca_2−CaM ($K_D = k_{10j}/k_{9j} < 100$ pM),[10,37,55−57] and the isolated C-terminal domain fragment of CaM also has very high affinity for many targets ($K_D < 1$ nM).[32] With such high affinities, even the highest measured association rate constants ($k_a = 10^8$ M^{-1} s^{-1}[32,56]) imply relatively low dissociation rate constants, $k_{off} = K_D/k_a < 0.1$ s^{-1}. The importance of intermediates is underscored by comparing the simulations at high Ca^{2+} oscillation frequency with those at very low frequency allowing dissociation of the intermediates between transients, under which conditions the level of differential activation is reduced (Figure 3). In some exceptional cases, such as the plasma membrane calcium pump, targets are activated by $CaM(Ca)_{2C}$,[58−60] but can, in competition with targets activated by $CaM(Ca)_4$, be regulated differentially by the kinetic mechanism described here, because dynamics in the CaM signaling network affect species having two Ca^{2+} ions bound.

Role of Calmodulin Concentration. The mechanism described here for differential activation does not depend directly on the stoichiometry between CaM and target protein. Thus, this mechanism can be responsible for differential activation even when there is a single target protein, as reflected in the frequency dependence of ΔP_j. However, the frequency dependence of the accumulation and depletion of intermediate species is enhanced by competition between targets for CaM. Competition is intensified by decreasing concentrations of CaM. Thus limiting CaM concentration enhances differential activation without being necessary for it.

Calmodulin Domain Structure. The results underscore the intricate optimization of CaM structure and function. The basis for hysteretic behavior in the network is the covalent coupling of two domains that bind Ca^{2+} sequentially, but with cooperativity in each domain, and that cooperate in target binding. The importance of paired sites in each domain is illustrated by the perturbation of target activation by mutations that deteriorate single EF-hands.[61] An important contribution to the essential hysteresis underlying the differential response is that CaM-target complexes with two Ca^{2+} ions bound may persist between transients but only complexes with four Ca^{2+} ions are active. This effect differs fundamentally from hysteresis due to accumulation of Ca^{2+} because of slow diffusion. Ca^{2+} accumulation can only increase the level of target activation, whereas accumulation of intermediates can also decrease the activation of some targets as illustrated by NOS. The high affinity and slow kinetics of Ca^{2+} binding to the C-terminal domain[37] explains why the $CaM(Ca)_{2C}P_j$ species play a pivotal role in activation of target proteins. The much higher affinity for Ca^{2+} compared to the more abundant Mg^{2+}, and the opposite domain preferences of Mg^{2+} and Ca^{2+}, are also critical and allow differential activation even at physiological Mg^{2+} concentrations.

Advantages of a Central Hub. The results underscore the many advantages of having the calmodulin signaling network centered on a common hub, calmodulin, as opposed to a signaling network composed of many Ca^{2+}-binding target proteins. A hub network facilitates coupling among network species by linking reactions involving different targets, making the whole network sensitive to the range of temporal dynamics of its most sensitive members. Distributed control would not allow the activation of some targets to suppress other ones one in a frequency sensitive manner, because they would not

dx.doi.org/10.1021/cn300218d | ACS Chem. Neurosci. 2013, 4, 601−612

compete for the same activator. A network centered on one common hub provides a mechanism for the cell to use Ca^{2+}-spike frequency to select which Ca^{2+}-regulated activities should be switched on at elevated Ca^{2+} concentration, as has indeed been found experimentally[62−64] and theoretically.[65]

Number of Targets. Increasing the number of target types increases the range of temporal dynamics the network can transduce into differential regulation. In the large-scale simulations, this is seen as a shift in the ΔA distribution toward higher values as the number of target types increases. The effects reported here have not saturated in networks with eight targets. Considering the large number of CaM target proteins found in eukaryotic cells,[11−23] the reported results are likely to underestimate the level of differential regulation *in vivo*. Importantly, the mechanism found here for differential activation would permit selective activation even of targets present in very low copy number, as the defining parameters are the rate constants. While association rate depends also on concentration, dissociation rate does not; thus even low copy number targets may build up a high fraction of inactive intermediates between transients.

Temporal versus Spatial Dynamics. The present study considers only temporal and not spatial dynamics in Ca^{2+} concentration. Slow diffusion of Ca^{2+} has been explored extensively as a mechanism for nonlinear activation of Ca^{2+}-dependent processes.[66] The low spatial resolution of experimental measurements, together with cytoplasmic heterogeneity, are obstacles for accurate modeling of spatial dynamics. However, for CaM target proteins that move slowly relative to the temporal dynamics of Ca^{2+}, such as immobilized or tethered targets or those that are part of large multiprotein complexes, spatial heterogeneity means that CaM targets in different locations experience different temporal dynamics. Thus, the different frequencies in the present simulations serve as a proxy for different locations. The kinetic mechanism described here is fully compatible with and may coexist with other mechanisms for signal modulation, such as alternative splicing of target proteins[67,68] and accumulation of Ca^{2+} in local microdomains.[9]

Stochasticity. The differential equations used here assume continuous concentrations, whereas the numbers of protein molecules and calcium ions are discrete and potentially small. A typical mammalian cell has a volume of 1 pL, which at the protein concentrations used in the simulations represents 6×10^5−6×10^8 molecules per cell. A simple measure of the effect of stochasticity is the counting error estimated as the coefficient of variation (CV) of Poisson distributions whose expectation values are in the range 6×10^5−6×10^8. At the low end of this range, CV is 0.001, and at the high end it is 4×10^{-5}. These values indicate that the continuous assumption underlying the use of differential equations is reasonable for the binding interactions modeled here.

Amplification from Opposing Activities. Some CaM targets have mutually opposing activities (e.g., adenylate cyclase and cAMP phosphodiesterases) or inhibit each other (e.g., CN and CaMK II). In such cases, modest ΔA values may be amplified by the dynamics of reciprocal inhibition and contribute to differential signal transduction. If CN activity is higher than CaMK II activity, CN will suppress CaMK II activation while at the same time relieving the inhibition of its own activation. Amplification may even result in bistable responses, such as the induction of long-term synaptic potentiation (LTP) and depression (LTD).

CONCLUSIONS

Differential target activation in the calmodulin signaling network can be regulated by the Ca^{2+} oscillation frequency. Differential activation increases with increasing numbers of targets and with decreasing CaM concentration. The underlying mechanism relies on the two-domain structure of CaM, the opposite binding preferences of the two domains for Ca^{2+} and Mg^{2+}, and differences in association and dissociation rates among target-CaM complexes. Given the generality of the model, it may be relevant to other oscillatory dynamics in signal transduction and transcriptional regulation.[69,70].

METHODS

Network Model. The network model (Figure 2) includes free Ca^{2+}, free target proteins, calmodulin (CaM) with zero, two or four Ca^{2+} bound, as well as target-bound CaM with zero, two, or four Ca^{2+} bound. With one target protein, the network thus contains 8 species (Ca^{2+}, CaM, $CaM(Ca)_{2C}$, $CaM(Ca)_4$, P_j, $CaMP_j$, $CaM(Ca)_{2C}P_j$, $CaM(Ca)_4P_j$) and 14 rate constants (Figure 2). Each additional target adds 4 species (P_j, $CaMP_j$, $CaM(Ca)_{2C}P_j$, $CaM(Ca)_4P_j$) and 10 rate constants to the network. Due to positive cooperativity of Ca^{2+} binding within each domain,[31] complexes of CaM with one or three Ca^{2+} ions bound will have much lower concentration (Figure 1D) and only those with zero, two or four Ca^{2+} ions bound are considered in the model. The lower affinity and faster dissociation of Ca^{2+} from the N-terminal domain make the concentrations of $CaM(Ca)_{2N}$ and $CaM(Ca)_{2N}P_j$ insignificant [37] and these species were not included in the model. In the initial simulations with two targets, the total concentrations of CaM and targets were all fixed at 5 μM. In larger-scale simulations with networks of two, four, or eight hypothetical targets, target concentrations were sampled from the range 1−100 μM, and CaM concentration in the ranges 1−10, 1−100, or 1−1000 μM.

Rate Equations. Differential mass-action equations (eq 1−5) and mass-balance equations (eq 6−8) describe the rates of conversion between species and species distribution. Each differential equation describes the rate of change in the concentration of one species and contains production terms accounting for the reactions that generate the species, and degradation terms accounting for the reactions that consume the species. The equations are written in a general form for the jth target protein (P_j) to model networks containing any number of targets. For n targets there are $2 + 3n$ differential equations and $1 + 2n$ mass balance equations.

$$\frac{d[CaM]}{dt} = \sum_{j=1}^{n} k_{6_j}[CaMP_j] + k_4[CaM(Ca)_{2C}] - [CaM](k_3[Ca^{2+}]^2 + \sum_{j=1}^{n} k_{5_j}[P_j]) \quad (1)$$

$$\frac{d[CaM(Ca)_{2C}]}{dt} = \sum_{j=1}^{n} k_{8_j}[CaM(Ca)_{2C}P_j] + k_3[CaM][Ca^{2+}]^2 + k_2[CaM(Ca)_4] - [CaM(Ca)_{2C}](k_1[Ca^{2+}]^2 + \sum_{j=1}^{n} k_{7_j}[P_j] + k_4) \quad (2)$$

$$\frac{d[CaMP_j]}{dt} = k_{5_j}[CaM][P_j] + k_{4_j}[CaM(Ca)_{2C}P_j] - [CaMP_j](k_{3_j}[Ca^{2+}]^2 + k_{6_j}) \quad (3)$$

dx.doi.org/10.1021/cn300218d | ACS Chem. Neurosci. 2013, 4, 601−612

$$\frac{d[CaM(Ca)_{2C}P_j]}{dt} = k_{3_j}[CaMP_j][Ca^{2+}]^2 + k_{7_j}[CaM(Ca)_{2C}][P_j] + k_{2_j}[CaM(Ca)_4P_j] - [CaM(Ca)_{2C}P_j](k_{4_j} + k_{1_j}[Ca^{2+}]^2 + k_{8_j}) \quad (4)$$

$$\frac{d[CaM(Ca)_4P_j]}{dt} = k_{9_j}[CaM(Ca)_4][P_j] + k_{1_j}[CaM(Ca)_{2C}][Ca^{2+}]^2 - [CaM(Ca)_4P_j](k_{2_j} + k_{10_j}) \quad (5)$$

$$[P_j]_{bound} = [CaMP_j] + [CaM(Ca)_{2C}P_j] + [CaM(Ca)_4P_j] \quad (6)$$

$$[CaM(Ca)_4] = C_{CaM}^{total} - \{\sum_{j=1}^{n}[P_j]_{bound} + [CaM(Ca)_{2C}] + [CaM]\} \quad (7)$$

$$[P_j] = C_{P_j}^{total} - [P_j]_{bound} \quad (8)$$

where $[Ca^{2+}]$ denotes free Ca^{2+} concentration, [CaM] the free CaM concentration, $[CaM(Ca)_{2C}]$ the concentration of CaM with two Ca^{2+} ions bound to its C-terminal domain, $[P_j]$ the free concentration of the jth target protein, and $[CaM(Ca)_iP_j]$ the concentration of the complex of CaM and the jth target protein having i Ca^{2+} ions bound.

Rate Constants. The binding of Ca^{2+} to CaM is described by four rate constants (k_1, k_2, k_3, and k_4; Figure 2) with values that have been reported by multiple laboratories (Table 1). Using eqs 9−12, two rate constants (k_{2j} and k_{4j}) were expressed in terms of the remaining eight rate constants. For nitric oxide synthase and calcineurin, some equilibrium and rate constants have been estimated experimentally;[10,55−57,71−73] their values and the sources of the rate constants are listed in Table 1. The association rate constants for Ca^{2+} binding to CaM complexed to these targets are unknown but could be calculated from the other values using eqs 11 and 12. These rate constants are listed in Table 1 as inferred. Equations 9 and 10 describe the thermodynamic cycles by which the binding reactions are linked; ΔG_C and $\Delta G_{P,C}$ are the free energy of Ca^{2+} binding to free and target-bound CaM, respectively, and ΔG_P and $\Delta G_{C,P}$ are the free energy of target binding to free and Ca^{2+}-bound CaM, respectively.

$$\Delta G_C + \Delta G_{C,P} = \Delta G_P + \Delta G_{P,C} \quad (9)$$

$$\Delta G_{C,N} + \Delta G_{CN,P} = \Delta G_{C,P} + \Delta G_{CP,N} \quad (10)$$

$$k_{2_j} = k_{7_j}\frac{k_{10_j}}{k_{9_j}}\frac{k_2}{k_1}\frac{k_{1_j}}{k_{8_j}} \quad (11)$$

$$k_{4_j} = k_{5_j}\frac{k_{8_j}}{k_{7_j}}\frac{k_4}{k_3}\frac{k_{3_j}}{k_{6_j}} \quad (12)$$

In larger scale simulations with generalized networks of two, four, or eight targets, the sets of rate constants for each target were sampled randomly from the log-scale ranges established by the upper and lower limits presented in Table 2. These limits were chosen to encompass the highest and the lowest values reported in the literature.[52,55] Each set of parameters was generated as follows. Each unknown rate constant, except k_{2j} and k_{4j}, was sampled randomly from the log range for its values, and the sampled values were used to compute k_{2j} and k_{4j}. Sets of rate constants were discarded if they correspond to target proteins with target affinity for $CaM(Ca)_4$ lower than that for $CaM(Ca)_2$; target affinity for $CaM(Ca)_2$ weaker than 10^5 M^{-1} (K_D > 10 μM); or Ca^{2+} affinity of the N-terminal CaM domain in target complexes greater than 10^7 M^{-1} (K_D < 0.1 μM).[32] Such targets cannot be regulated by Ca^{2+} transients because CaM-target complexes would be more than half-saturated even at basal concentrations of free Ca^{2+} (~0.1 μM).

Ca^{2+}-Concentration Profile. A train of Ca^{2+} spikes was generated as a piece-wise continuous function as follows.

During intertransient intervals: $[Ca^{2+}] = 0.1$ μM

During transient: $[Ca^{2+}] = (0.1 + 0.9\sin(\omega\{t - \tau(i)\})^n)$ μM

$\tau(i)$ is the start position of the ith transient in the train. This yields trains of identical Ca^{2+} transients with peak $[Ca^{2+}]$ = 1 μM separated by intertransient periods with $[Ca^{2+}]$ = 0.1 μM, closely resembling the experimentally measured profiles.[5,6] Each transient lasted for one-half-period of the sine wave, and the midheight duration is $t_{1/2} = 2\omega^{-1}[\arcsin(1) - \arcsin(2^{-1/n})]$. This work used ω = 10 and n = 2 yielding $t_{1/2}$ = 157 ms, or ω = 20 and n = 4 yielding $t_{1/2}$ = 57 ms.

Simulations. To investigate the activation of CaM target proteins in response to the train of Ca^{2+} transients, the evolution of the different species in the network was calculated using eqs 1−8. The system of coupled differential equations was integrated using numerical and backward differentiation formulas[74] with adaptive time steps ranging from 10 fs to 10 ms. In test simulations of networks with two target proteins, the numerical integration was performed with a modified Rosenbrock formula of order 2 (ref 74) and gave the same results, indicating numerical convergence and to the absence of large systematic errors.

Including Mg^{2+}. The binding of Mg^{2+} was modeled in analogy with the binding of Ca^{2+}. The Ca^{2+} and Mg^{2+} networks are coupled by the following elementary reactions involving mixed species with both Ca^{2+} and Mg^{2+}.

$$CaM(Mg)_{2N} + 2Ca^{2+} \underset{k_4}{\overset{k_3}{\rightleftharpoons}} CaM(Mg)_{2N}(Ca)_{2C}$$

$$CaM(Ca)_{2C} + 2Mg^{2+} \underset{k_4^m}{\overset{k_3^m}{\rightleftharpoons}} CaM(Mg)_{2N}(Ca)_{2C}$$

$$CaM(Mg)_{2N}P_j + 2Ca^{2+} \underset{k_{4_j}}{\overset{k_{3_j}}{\rightleftharpoons}} CaM(Mg)_{2N}(Ca)_{2C}P_j$$

$$CaM(Ca)_{2C}P_j + 2Mg^{2+} \underset{k_{4_j}^m}{\overset{k_{3_j}^m}{\rightleftharpoons}} CaM(Mg)_{2N}(Ca)_{2C}P_j$$

Dissociation of Mg^{2+} from the N-terminal sites may be rate limiting for binding of Ca^{2+}, and is described by the combination of elementary reactions. The species $CaM(Mg)_{2C}$ and $CaM(Mg)_{2C}(Ca)_{2N}P_j$ were not included because Mg^{2+} has opposite preference for the two domains of CaM compared to Ca^{2+} and competes for the N-terminal domain only. As found experimentally, the binding of Mg^{2+} to one CaM domain does not change the affinity of the other domain for Ca^{2+} or the affinity of CaM for target protein.[35] By thermodynamic linkage, the presence of targets does not alter the affinity of CaM for Mg^{2+}. Thus, the rate constants for binding of a target are assumed to be unaffected by Mg^{2+} binding, and the rate constants for the binding of Mg^{2+} to one domain are not altered by the binding Ca^{2+} to the other domain or by the binding of targets. These assumptions reduce to four the number of new rate constants needed to include Mg^{2+}. The values used for these four constants are found in Table 3.

Metrics for Differential Activation. Two metrics ΔP_j (eq 13) and ΔA (eq 14) are defined to quantify differential activation in the large-scale simulations. Two oscillations are compared that have eleven identical Ca^{2+} transients and differ only in the time intervals between successive Ca^{2+} transients.

Table 3. Rate Constants for Mg^{2+}[a]

k_a/mM^{-1}s^{-1}	k_d/s^{-1}
k_1^m = 172	k_2^m = 380
k_3^m = 127	k_4^m = 1635

[a]Rate constants for association and dissociation of Mg^{2+} from ref 34 and 35. For notation see Supporting Information Figure S3.

dx.doi.org/10.1021/cn300218d | ACS Chem. Neurosci. 2013, 4, 601−612

$$\Delta P_j = 1 + \frac{\int_0^{t_1}(C_j^{T_1} - C_j^B)\,dt - \int_0^{t_2}(C_j^{T_2} - C_j^B)\,dt}{\min[\int_0^{t_1}(C_j^{T_1} - C_j^B)\,dt \int_0^{t_1}(C_j^{T_2} - C_j^B)\,dt]} \quad (13)$$

$$\Delta A = \frac{1}{n}\sum_{j=1}^{j=n} |\Delta P_j| \quad (14)$$

ΔP_j quantifies the fold increase in the activation of the jth target protein (P_j) as a function of the intertransient periods T_1 and T_2. ΔA is the arithmetic average of the absolute values of ΔP_j for all CaM target proteins included in the simulation. $C_j^{T_1}$, $C_j^{T_2}$, and C_j^B are the concentrations of active complexes, $CaM(Ca)_4P_j$, during transients with periods T_1 and T_2, and at basal $[Ca^{2+}] = 0.1\ \mu M$, and n is the number of target proteins in the network. t_1 and t_2 are the durations of the trains of transients (oscillations) with frequencies $1/T_1$ and $1/T_2$, respectively. $t_1T_1 = t_2T_2$, that is, the number of Ca^{2+} transients, is the same for both frequencies.

Sensitivity Analysis. Partial correlations were calculated between ΔA and each parameter ($\boldsymbol{\alpha_1}$) for the 10 rate constants k_{1j}–k_{10j} and the total concentrations of CaM (C_1) and target proteins (C_2), as well as between ΔA and each pair of parameters ($\boldsymbol{\alpha_2}$):

$$\mathbf{P}\boldsymbol{\alpha_1} = \mathbf{dA} \rightarrow \boldsymbol{\alpha_1} = (\mathbf{P^TP})^{-1}(\mathbf{P^TdA}) \quad (15)$$

$$\mathbf{Q}\boldsymbol{\alpha_2} = \mathbf{dA} \rightarrow \boldsymbol{\alpha_2} = (\mathbf{Q^TQ})^{-1}(\mathbf{Q^TdA}) \quad (16)$$

P is a matrix in which each column corresponds to a parameter and each row is a simulated set of parameters. **dA** is a vector with the corresponding values of differential activation. Each column of **P** contains the Z-scores of one parameter, meaning the simulated values of that parameter normalized to have zero mean and unit variance to permit comparison on the same scale of parameters with orders-of-magnitude differences in their dynamic ranges. Similar to **P**, **Q** is a matrix containing all pairwise products of parameters, for example, the first column is the Z-score (normalized to zero mean and unit variance) of the element-wise product of the first and second columns of **P**, the second column of **Q** is the Z-score of the pairwise product of the first and the third columns in **P** and so on. This overdetermined linear system (in the least-squares sense) is solved for $\boldsymbol{\varepsilon_1}$ and $\boldsymbol{\varepsilon_2}$, the vectors of partial correlations. The interdependence between a pair of parameters (say, i and j) is measured by the difference between the $\boldsymbol{\varepsilon_2}$ element corresponding to i and j and the product of $\boldsymbol{\varepsilon_1}$ elements corresponding to i and j. This approach is a simplification that decomposes a nonlinear dependence into a set of component functions (second order polynomials), which approximate the influence of each parameter on the level of differential activation.

■ ASSOCIATED CONTENT

Ⓢ Supporting Information

Additional figures as described in the text. This material is available free of charge via the Internet at http://pubs.acs.org.

■ AUTHOR INFORMATION

Corresponding Author

*E-mail: Sara.Linse@biochemistry.lu.se.

Present Address

‖N.S.: Massachusetts Institute of Technology, Cambridge, MA 02139, USA.

Funding

This work was supported by the Crafoord Foundation, Lund (S.L.), Swedish Research Foundation (S.L.), and the Linneaus Centre Organizing Molecular Matter (S.L., J.C.).

Notes

The authors declare no competing financial interest.

■ ACKNOWLEDGMENTS

We thank R. J. P. Williams, R.H. Kretsinger, and Ned Wingreen for their insightful comments on the manuscript. The help with typing by Ingrid Hughes is gratefully acknowledged.

■ REFERENCES

(1) Kupzig, S., Walker, S. A., and Cullen, P. J. (2005) The frequencies of calcium oscillations are optimized for efficient calcium-mediated activation of ras and the ERK/MAPK cascade. *Proc. Natl. Acad. Sci. U.S.A. 102*, 7577−7582.

(2) Dolmetsch, R. E., Xu, K., and Lewis, R. S. (1998) Calcium oscillations increase the efficiency and specificity of gene expression. *Nature 392*, 933−936.

(3) Saucerman, J. J., and Bers, D. M. (2008) Calmodulin mediates differential sensitivity of CaMKII and calcineurin to local Ca2+ in cardiac myocytes. *Biophys. J. 95*, 4597−4612.

(4) Berridge, M. J. (2012) Calcium signalling remodelling and disease,,. *Biochem. Soc. Trans. 40*, 297−309.

(5) Berridge, M. J., Bootman, M. D., and Roderick, H. L. (2003) Calcium signalling: dynamics, homeostasis and remodelling. *Nat. Rev. Mol. Cell. Biol. 4*, 517−529.

(6) Berridge, M. J. (2005) Unlocking the secrets of cell signaling. *Annu. Rev. Physiol. 67*, 1−21.

(7) Ng, C. K., and McAinsh, M. R. (2003) Encoding specificity in plant calcium signalling: hot-spotting the ups and downs and waves. *Ann. Bot. 92*, 477−485.

(8) Tran, Q. K., Black, D. J., and Persechini, A. (2005) Dominant affectors in the calmodulin network shape the time courses of target responses in the cell. *Cell Calcium 37*, 541−553.

(9) Naoki, H., Sakumura, Y., and Ishii, S. (2005) Local signaling with molecular diffusion as a decoder of Ca2+ signals in synaptic plasticity. *Mol. Syst. Biol. 1*, 2005.0027.

(10) Stefan, M. I., Edelstein, S. J., and Le Novère, N. (2008) An allosteric model of calmodulin explains differential activation of PP2B and CaMKII. *Proc. Natl. Acad. Sci. U.S.A. 105*, 10768−10773.

(11) Yap, K. L., Kim, J., Truong, K., Sherman, M., Yuan, T., and Ikura, M. (2000) Calmodulin target database. *J. Struct. Funct. Genomics 1*, 8−14.

(12) Zhu, H., Bilgin, M., Bangham, R., Hall, D., Casamayor, A., Bertone, P., Lan, N., Jansen, R., Bidlingsmaier, S., Houfek, T., Mitchell, T., Miller, P., Dean, R. A., Gerstein, M., and Snyder, M. (2001) Global analysis of protein activities using proteome chips. *Science 293*, 2101−2105.

(13) Ikura, M., Osawa, M., and Ames, J. B. (2002) The role of calcium-binding proteins in the control of transcription: structure to function. *Bioessays 24*, 625−636.

(14) Kahl, C. R., and Means, A. R. (2003) Regulation of cell cycle progression by calcium/calmodulin-dependent pathways. *Endocr. Rev. 24*, 719−736.

(15) Shen, X., Valencia, C. A., Szostak, J. W., Dong, B., and Liu, R. (2005) Scanning the human proteome for calmodulin-binding proteins. *Proc. Natl. Acad. Sci. U. S. A. 102*, 5969−5974.

(16) Xia, Z., and Storm, D. R. (2005) The role of calmodulin as a signal integrator for synaptic plasticity. *Nat. Rev. Neurosci. 6*, 267−276.

(17) Berggård, T., Arrigoni, G., Olsson, O., Fex, M., Linse, S., and James, P. (2006) 140 mouse brain proteins identified by Ca2+-calmodulin affinity chromatography and tandem mass spectrometry. *J. Proteome Res. 5*, 669−687.

(18) Clapham, D. E. (2007) Calcium Signaling. *Cell 131*, 1047−1058.

(19) Popescu, S. C., Popescu, G. V., Bachan, S., Zhang, Z., Seay, M., Gerstein, M., Snyder, M., and Dinesh-Kumar, S. P. (2007) Differential binding of calmodulin-related proteins to their targets revealed through high-density Arabidopsis protein microarrays. *Proc. Natl. Acad. Sci. U.S.A. 104*, 4730−4735.

(20) Calabria, L. K., Garcia Hernandez, L., Teixeira, R. R., Valle de Souza, M., and Espindola, F. S. (2008) Identification of calmodulin-binding proteins in brain of worker bees. *Comp. Biochem. Physiol., Part B: Biochem. Mol. Biol. 15*, 41−45.

(21) Bauer, M. C., O'Connell, D., Cahill, D. J., and Linse, S. (2008) Calmodulin binding to the polybasic C-termini of STIM proteins involved in store-operated calcium entry. *Biochemistry 47*, 6089−6091.
(22) Shen, X., Valencia, C. A., Gao, W., Cotten, S. W., Dong, B., HUang, B. C., and Liu, R. (2008) Ca2+/Calmodulin binding proteins from the C. elegans proteome. *Cell Calcium 43*, 444−456.
(23) O'Connell, D. J., Bauer, M. C., O'Brien, J., Johnson, W. M., Divizio, C. A., O'Kane, S. L., Berggård, T., Merino, A., Åkerfeldt, K. S., Linse, S., and Cahill, D. J. (2010) Integrated protein array screening and high throughput validation of 70 novel neural calmodulin-binding proteins. *Mol. Cell Proteomics 9*, 1118−1132.
(24) O'Connell, D. J. Bauer, M., Marshall, C., Ikura, M., and Linse, S. (2013) Calmodulin. In *Encylopedia of Metalloproteins* (Kretsinger, Uversky, and Permyakov, Eds.), Springer.
(25) Hoeflich, K. P., and Ikura, M. (2002) Calmodulin in action: diversity in target recognition and activation mechanisms. *Cell 108*, 739−742.
(26) Kawasaki, H., Nakayama, S., and Kretsinger, R. H. (1998) Classification and evolution of EF-hand proteins. *Biometals 11*, 277−295.
(27) Moncrief, N. D., Kretsinger, R. H., and Goodman, M. (1990) Evolution of EF-hand calcium-modulated proteins. I. Relationships based on amino acid sequences. *J. Mol. Evol. 30*, 522−562.
(28) Wang, B., Martin, S. R., Newman, R. A., Hamilton, S. L., Shea, M. A., Bayley, P. M., and Beckingham, K. M. (2004) Biochemical properties of V91G calmodulin: A calmodulin point mutation that deregulates muscle contraction in Drosophila. *Protein Sci. 13*, 3285−3297.
(29) Persechini, A., and Kretsinger, R. H. (1998) The central helix of calmodulin functions as a flexible tether. *J. Biol. Chem. 263*, 12175−12178.
(30) Chou, J. J., Li, S., Klee, C. B., and Bax, A. (2001) Solution structure of Ca(2+)-calmodulin reveals flexible hand-like properties of its domains. *Nat. Struct. Biol. 8*, 990−997.
(31) Linse, S., Helmersson, A., and Forsén, S. (1991) Calcium binding to calmodulin and its globular domains. *J. Biol. Chem. 266*, 8050−8054.
(32) Peersen, O. B., Madsen, T. S., and Falke, J. J. (1997) Intermolecular tuning of calmodulin by target peptides and proteins: Differential effects on Ca^{+2} binding and implications for kinase activation. *Protein Sci. 6*, 794−807.
(33) Martin, S. R., Andersson Teleman, A., Bayley, P. M., Drakenberg, T., and Forsén, S. (1985) Kinetics of calcium dissociation from calmodulin and its tryptic fragments. A stopped-flow fluorescence study using Quin 2 reveals a two-domain structure. *Eur. J. Biochem. 151*, 543−550.
(34) Malmendal, A., Evenäs, J., Thulin, E., Gippert, G. P., Drakenberg, T., and Forsén, S. (1998) When Size Is Important. *J. Biol. Chem. 273*, 28994−29001.
(35) Martin, S. R., Masino, L., and Bayley, P. M. (2000) Enhancement by Mg^{2+} of domain specificity in Ca?$^{+}$-dependent interactions of calmodulin with target sequences. *Protein Sci. 9*, 2477−2488.
(36) Malmendal, A., Linse, S., Evenäs, J., Forsén, S., and Drakenberg, T. (1999) Battle for the EF-hands: Magnesium-Calcium Interference in Calmodulin. *Biochemistry 38*, 11844−11850.
(37) Bayley, P. M., Findlay, W. A., and Martin, S. R. (1996) Target recognition by calmodulin: Dissecting the kinetics and affinity of interaction using short peptide sequences. *Protein Sci. 5*, 1215−1228.
(38) Linse, S., Drakenberg, T., and Forsén, S. (1986) Mastoparan binding induces a structural change affecting both the N-terminal and C-terminal domains of calmodulin. A 113Cd-NMR study. *FEBS Lett. 199*, 28−32.
(39) Ikura, M., Clore, G. M., Gronenborn, A. M., Zhu, G., Klee, C. B., and Bax, A. (1992) Solution structure of a calmodulin-target peptide complex by multidimensional NMR. *Science 256*, 632−638.
(40) Meador, W. E., Means, A. R., and Quiocho, F. A. (1992) Target enzyme recognition by calmodulin: 2.4 A structure of a calmodulin-peptide complex. *Science 257*, 1251−1255.
(41) Stigler, J., Ziegler, F., Gieseke, A., Gebhardt, J. C., and Rief, M. (2011) The complex folding network of single calmodulin molecules. *Science 334*, 512−516.
(42) André, I., Kesvatera, T., Jönsson, B., Åkerfeldt, K. S., and Linse, S. (2004) The role of electrostatic interactions in calmodulin-peptide complex formation. *Biophys. J. 87*, 1929−1938.
(43) André, I., Kesvatera, T., Jönsson, B., and Linse, S. (2006) Salt enhances calmodulin-target binding. *Biophys. J. 90*, 2903−2910.
(44) Hellstrand, E., Kukora, S., Shuman, C. F., Steenbergen, S., Thulin, E., Kohli, A., Krouse, B., Linse, S., and Åkerfeldt, K. S. FRET studies of calmodulin produced by native protein ligation reveal inter-domain electrostatic repulsion. Submitted.
(45) Yamniuk, A. P., and Vogel, H. J. (2004) Calmodulin's flexibility allows for promiscuity in its interactions with target proteins and peptides. *Mol. Biotechnol. 27*, 33−57.
(46) Osawa, M., Swindells, M. B., Tanikawa, J., Tanaka, T., Mase, T., Furuya, T., and Ikura, M. (1998) Solution structure of calmodulin-W-7 complex: the basis of diversity in molecular recognition. *J. Mol. Biol. 276*, 165−176.
(47) Linse, S., Voorhies, M., Norström, E., and Schultz, D. A. (2000) An EF-hand phage display study of calmodulin subdomain pairing. *J. Mol. Biol. 296*, 473−486.
(48) Shuman, C., Jiji, R., Åkerfeldt, K. S., and Linse, S. (2006) Reconstitution of calmodulin from domains and subdomains: Influence of target peptide. *J. Mol. Biol. 358*, 870−881.
(49) Chin, D., and Means, A. R. (2000) Calmodulin: a prototypical calcium sensor. *Trends Cell Biol. 10*, 322−328.
(50) Kakiuchi, S., Yasuda, S., Yamazaki, R., Teshima, Y., Kanda, K., Kakiuchi, R., and Sobue, K. (1982) Quantitative determinations of calmodulin in the supernatant and particulate fractions of mammalian tissues. *J. Biochem. 92*, 1041−1048.
(51) Bhalla, U. S. (2002) Biochemical Signaling Networks Decode Temporal Patterns of Synaptic Input. *J. Comput. Neurosci. 13*, 49−62.
(52) Rubin, J. E., Gerkin, R. C., Bi, G. Q., and Chow, C. C. (2005) Calcium Time Course as a Signal for Spike-Timing−Dependent Plasticity. *J. Neurophysiol. 93*, 2600−2613.
(53) Nordell, P., Westerlund, F., Wilhelmsson, L. M., Nordén, B., and Lincoln, P. (2007) Kinetic recognition of AT-rich DNA by Ruthenium Complexes. *Angew. Chem., Int. Ed. 46*, 2203−2206.
(54) Linse, S., and Linse, B. (2007) Protein folding through kinetic discrimination. *J. Am. Chem. Soc. 129*, 8481−8486.
(55) Zhang, M., and Vogel, H. J. (1994) Characterization of the calmodulin-binding domain of rat cerebellar nitric oxide synthase. *J. Biol. Chem. 269*, 981−985.
(56) Waxham, M. N., Tsai, A. L., and Putkey, J. A. (1998) A mechanism for calmodulin (CaM) trapping by cam-kinase ii defined by a family of cam-binding peptides. *J. Biol. Chem. 273*, 17579−17584.
(57) Quintana, A. R., Wang, D., Forbes, J. E., and Waxham, M. N. (2005) Kinetics of calmodulin binding to calcineurin. *Biochem. Biophys. Res. Commun. 334*, 674−680.
(58) Guerini, D., Krebs, J., and Carafoli, E. (1984) Stimulation of the purified erythrocyte Ca2+-ATPase by tryptic fragments of calmodulin. *J. Biol. Chem. 259*, 15172−15177.
(59) Elshorst, B., Hennig, M., Försterling, H., Diener, A., Maurer, M., Schulte, P., Schwalbe, H., Griesinger, C., Krebs, J., Schmid, H., Vorherr, T., and Carafoli, E. (1999) NMR solution structure of a complex of calmodulin with a binding peptide of the Ca^{2+} pump. *Biochemistry 38*, 12320−12332.
(60) Bayer, K. U., De Koninck, P., and Schulman, H. (2002) Alternative splicing modulates the frequency-dependent response of CaMKII to Ca(2+) oscillations. *EMBO J. 21*, 3590−3597.
(61) Gao, Z. H., Krebs, J., VanBerkum, M. F., Tang, W. J., Maune, J. F., Means, A. R., Stull, J. T., and Beckingham, K. (1993) Activation of four enzymes by two series of calmodulin mutants with point mutations in individual Ca2+ binding sites. *J. Biol. Chem. 268*, 20096−20104.
(62) De Koninck, P., and Schulman, H. (1998) Sensitivity of CaM kinase II to the frequency of Ca2+ oscillations. *Science 279*, 227−230.

(63) Dupont, G., Houart, G., and De Koninck, P. (2003) Sensitivity of CaM kinase ii to the frequency of CaM oscillations: a simple model. *Cell. Calcium 34*, 485−497.
(64) Bradshaw, J. M., Kubota, Y., Meyer, T., and Schulman, H. (2003) An ultrasensitive Ca^{2+}/calmodulin-dependent protein kinase Il protein phosphatase 1 switch facilitates specificity in postsynaptic calcium signaling. *Proc. Natl. Acad. Sci. U.S.A. 100*, 10512−10517.
(65) Gall, D., Baus, E., and Dupont, G. (2000) Activation of the liver glycogen phosphorylase by Ca^{2+} oscillations: a theoretical study. *J. Theor. Biol. 207*, 445−454.
(66) Naoki, H., Sakumura, Y., and Ishii, S. (2005) Local signaling with molecular diffusion as a decoder of Ca2+ signals in synaptic plasticity. *Mol. Syst. Biol. 1*, 2005.0027.
(67) Strehler, E. E., and Zacharias, D. A. (2001) Role of alternative splicing in generating isoform diversity among plasma membrane calcium pumps. *Physiol. Rev. 81*, 21−50.
(68) Brini, M. (2009) Plasma membrane Ca(2+)-ATPase: from a housekeeping function to a versatile signaling role. *Pflugers Arch. 457*, 657−664.
(69) Hao, N., and O'Shea, E. K. (2012) Signal-dependent dynamics of transcription factor translocation controls gene expression. *Nat. Struct. Mol. Biol. 19*, 31−39.
(70) Slavov, N., Macinskas, J., Caudy, A., and Botstein, D. (2011) Metabolic cycling without cell division cycling in respiring yeast. *Proc. Natl. Acad. Sci. U. S. A. 108*, 19090−19095.
(71) Hashimoto, Y., and Soderling, T. (1989) Regulation of calcineurin by phosphorylation. Identification of the regulatory site phosphorylated by Ca^{+2}/calmodulin-dependent protein kinase II and protein kinase C. *J. Biol. Chem. 264*, 16524−16529.
(72) Perrino, B. A., Ng, L. Y., and Soderling, T. R. (1995) Calcium regulation of calcineurin phosphatase activity by its B subunit and calmodulin. *J. Biol. Chem. 270*, 340−346.
(73) Persechini, A., White, H. D., and Gansz, K. J. (1996) Different mechanisms for Ca^{2+} dissociation from complexes of calmodulin with nitric oxide synthase or myosin light chain kinase. *J. Biol. Chem. 271*, 62−67.
(74) Shampine, F. L., and Reichelt, M. W. (1997) The MATLAB ODE Suite. *SIAM J. Sci. Comput. 18*, 1−22.
(75) Koradi, R., Billeter, M., and Wüthrich, K. (1996) MOLMOL: a program for display and analysis of macromolecular structures. *J. Mol. Graphics 14*, 29−32.

■ NOTE ADDED AFTER ASAP PUBLICATION

This paper was published on the Web on February 5, 2013, with a missing operator from the last term in eq 2. The corrected version was reposted on February 12, 2013.